RECENT PROGRESS OF 1-MW BEAM TUNING IN THE J-PARC 3-GeV RCS

H. Hotchi#, H. Harada, S. Kato, M. Kinsho, K. Okabe, P. K. Saha, Y. Shobuda, F. Tamura, N. Tani, Y. Watanabe, K. Yamamoto, and M. Yoshimoto
J-PARC center, Japan Atomic Energy Agency, Tokai, Naka, Ibaraki, 319-1195 Japan

Abstract

This paper presents the recent progress of 1-MW beam tuning in the J-PARC 3-GeV RCS, especially focusing on our approaches to beam loss issues.

INTRODUCTION

The J-PARC 3-GeV rapid cycling synchrotron (RCS) is the world's highest class of high-power pulsed proton driver aiming for an output beam power of 1 MW. The injector linac delivers a 400-MeV H^- beam to the RCS injection point, where it is multi-turn charge-exchange injected through a 350-μg/cm^2-thick carbon foil over a period of 0.5 ms. RCS accelerates the injected protons up to 3 GeV with a repetition rate of 25 Hz, alternately providing the 3-GeV proton beam to the material and life science experimental facility and to the following 50-GeV main ring synchrotron by switching the beam destination pulse by pulse.

After completing injector linac upgrades, RCS started a 1-MW beam test in October 2014, and successfully achieved a 1-MW beam acceleration in January 2015. Since then, a large fraction of our effort has been focused on reducing and managing beam losses. This paper presents the recent progress of 1-MW beam tuning, especially focusing on our approaches to beam loss issues.

1-MW BEAM TEST CONDUCTED AFTER THE RF POWER SUPPLY UPGRADE

As already reported in the last IPAC [1], RCS achieved a 1-MW beam acceleration with no remarkable beam loss in January 2015, but then there still remained slight longitudinal beam loss ($<10^{-3}$) due to a limitation of the RF power supply. The longitudinal beam loss can cause excess machine activations in the high dispersion area if the continuous beam operation is carried out as is. But it was completely removed by beam loading compensation [2] conducted in October, 2015 after the RF power supply upgrade [3], as shown in Fig. 1.

After the RF power supply upgrade, most of the remaining beam loss was well localized at the collimator section. Figure 2 shows beam loss monitor (BLM) signals at the collimator measured for the first 4 ms with various beam intensities of up to 1 MW. As shown in the figure, the beam loss appears only for the first 1 ms, and the beam loss amount simply shows a linear beam intensity dependence. They indicate the observed beam loss mainly arises from foil scattering during charge-exchange injection. The other beam loss, such as space-charge induced beam loss, was well minimized by the combination of transverse and longitudinal painting [4-6]. The beam loss for the 1-MW beam was estimated to be ~0.1%. This corresponds to 130 W in power, which is much less than the collimator limit of 4 kW.

#hotchi.hideaki@jaea.go.jp

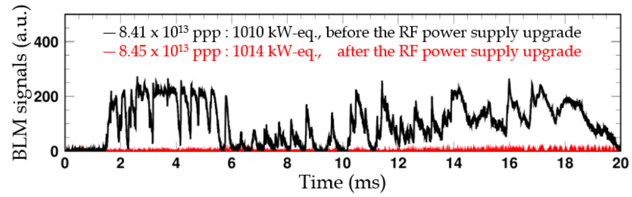

Figure 1: BLM signals in the high dispersion area measured over the whole 20 ms with a beam intensity of 1 MW before and after the RF power supply upgrade.

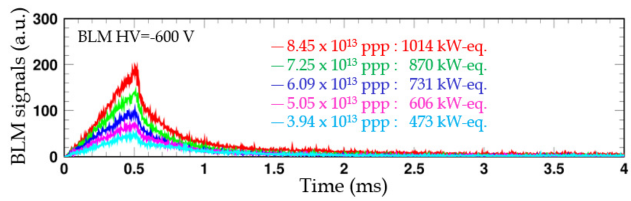

Figure 2: BLM signals at the collimator measured for the first 4 ms with various beam intensities of up to 1 MW, where 100π-mm-mrad correlated transverse painting and full longitudinal painting were applied.

FURTHER BEAM LOSS MITIGATION BY LARGER TRANSVERSE PAINTING

Beam loss other than foil scattering beam loss was well minimized. Thus the next subject is to further reduce the foil scattering beam loss. Most of the foil scattering beam loss is well localized at the collimators, so no serious problem has been encountered to date. But some of them with large scattering angles causes un-localized beam loss, making relatively high machine activations near the charge-exchange foil. It was 15 mSv/h on the chamber surface right after the 400-kW routine beam operation. This value should be 38 mSv/h if the output beam power is increased to 1 MW as is. To preserve a better hands-on-maintenance environment, the machine activation has to be reduced as low as possible. The amount of the foil scattering beam loss is in proportion to the foil hitting rate during injection. One possible solution to reduce the foil hitting rate is to expand the transverse painting area.

As described in [4], in RCS, horizontal painting is performed by a horizontal closed orbit variation during

ISBN 978-3-95450-147-2

injection. Thus the foil hitting rate decreases as the horizontal painting area becomes wider, because the circulating beam more rapidly escapes from the foil thanks to the larger horizontal closed orbit variation. On the other hand, vertical painting is performed by a vertical injection angle change during injection. Vertical painting also acts to reduce the foil hitting rate through the wider painting area than the vertical dimension of the foil. The painting emittance used thus far is 100π mm mrad, where the average number of foil hits per particle is 41. This number can be reduced to 25 or 15 if the painting emittance is enlarged to 150 or 200π mm mrad. But such a large transverse painting had not been realized until recently due to edge focusing additionally generated when the horizontal local orbit bump is active for beam injection. The edge focus causes 30% big beta function beating on the vertical plane. This beta function beating makes a distortion of the lattice super-periodicity and additionally excites various random betatron resonances during injection. Such random resonances cause a shrinkage of the dynamic aperture during the injection period, and leads to extra beam loss when the transverse painting area is enlarged.

To compensate the beta function beating, we recently installed 6 sets of pulse type quadrupole correctors (QDT) [7], by which the effect of the random resonances can be minimized through the recovery of the super-periodic condition. To confirm the effectiveness of the correction scheme, we performed a beam test with an 850-kW intensity beam [8]. As shown in Fig. 3, 0.5% significant extra beam loss occurred when the transverse painting area was enlarged from 100 to 150π mm mrad, but the beam loss was minimized as expected by applying QDTs.

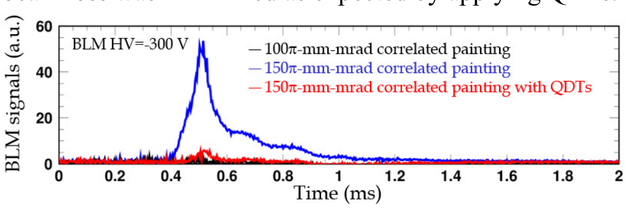

Figure 3: BLM signals at the collimator measured for the first 2 ms with a beam intensity of 850 kW.

The experimental result was well reproduced by the corresponding numerical simulation. We investigated more detailed mechanism for the observed phenomena using the numerical simulation result [8]. Figure 4 shows a tune diagram near the present operating point. The numerical simulation confirmed the observed extra beam loss is generated through vertical beam halo formation caused by the combined effect of two resonances; $\nu_x+2\nu_y=19$ and $2\nu_x-2\nu_y=0$. The $\nu_x+2\nu_y=19$ resonance is a third-order random resonance arising from the chromatic correction sextupole field and the intrinsic sextupole field component in the main bending magnets, and it is additionally excited through a distortion of the super-periodicity caused by the edge focus during injection. This sum resonance induces emittance growth on both horizontal and vertical planes with the invariant value of $2J_x-J_y$. On the other hand, the $2\nu_x-2\nu_y=0$ resonance is a fourth-order systematic resonance, which is mainly excited through the octupole component in the space charge field. This difference resonance induces emittance exchange between the horizontal and the vertical planes with the invariant value of J_x+J_y. Figure 5 shows a typical sample of the turn-by-turn betatron actions of one macro-particle that forms beam loss. In this figure, one can see a characteristic emittance blow-up that implies the combined effect of the two resonances; the horizontal and the vertical actions of the macro-particle gradually grow up along the line of $2J_x-J_y$ =const, while oscillating in a direction parallel to the line of J_x+J_y=const. This analysis confirmed that most of the observed beam loss is generated through such a single-particle behaviour. In particular, the contribution of the $\nu_x+2\nu_y=19$ resonance is more critical, since the resonance causes more severe beam halo formation on the vertical plane. QDTs act to mitigate the $\nu_x+2\nu_y=19$ resonance through the recovery of the super-periodic condition. That is, it follows that the beam loss reduction achieved in this beam test is led through the beam halo mitigation by QDTs.

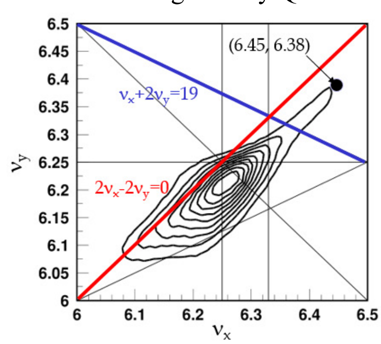

Figure 4: Tune diagram near the present operating point, where the tune footprint was calculated at the end of injection with 150π-mm-mrad correlated painting assuming a beam intensity of 850 kW.

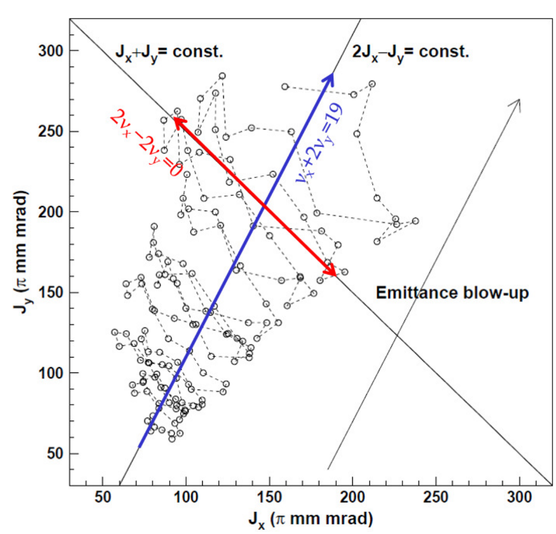

Figure 5: 2D plot of the turn-by-turn betatron actions of one macro-particle that forms beam loss.

ISBN 978-3-95450-147-2

The above analysis also suggests that the further expansion of transverse painting area can be realized by reducing the effect of the $2\nu_x-2\nu_y=0$ resonance as well as mitigating the $\nu_x+2\nu_y=19$ resonance with QDTs. For this clue, we discussed the introduction of anti-correlated painting, instead of correlated painting used thus far. Anti-correlated painting has several advantages for mitigating the effect of the $2\nu_x-2\nu_y=0$ resonance. In RCS, both correlated and anti-correlated painting are available. As shown in the left plot in Fig. 6, in correlated painting, the injection beam is painted along the blue arrow. To the direction of beam painting, the emittance exchange by the $2\nu_x-2\nu_y=0$ resonance occurs in the orthogonal direction like the red arrow. Thus the emittance exchange is directly connected to the emittance growth in this case. On the other hand, in anti-correlated painting, the direction of beam painting is the same as the direction of the emittance exchange as shown in the right plot in Fig. 6. Therefore, the emittance growth caused by the emittance exchange is well suppressed in this case. Another advantage of anti-correlated painting is to make a KV-like distribution. Therefore anti-correlated painting gives less space-charge octupole field component, so it acts to mitigate the $2\nu_x-2\nu_y=0$ resonance.

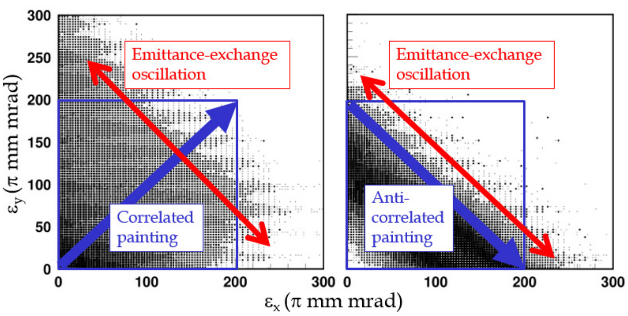

Figure 6: 2D plot of the beam emittances calculated at the end of injection with 200π-mm-mrad correlated and anti-correlated painting assuming a beam intensity of 1 MW.

Based on the above considerations, we tried to further expand the transverse painting area to 200π mm mrad for the 1-MW beam. Figure 7 shows the experimental result. The first plot (a) is the case of 200π-mm-mrad correlated painting, where 1.9% significant extra beam loss occurred. The beam loss was reduced to (b) as expected by introducing anti-correlated painting. The beam loss was further reduced to (c) by turning off the chromaticity correction, that is, by turning off the sextupole magnets. Less sextupole field mitigates the effect of the $\nu_x+2\nu_y=19$ resonance, which is the main cause of this beam loss reduction. The beam loss was finally reduced to (d) by introducing QDTs, which is caused by the further mitigation of the $\nu_x+2\nu_y=19$ resonance through the recovery of the lattice super-periodicity. As shown in the plot (d), slight extra beam loss still remains. But we expect the remaining beam loss does not lead to serious issue, because the value is small enough; besides most of the beam loss can be localized at the collimator section. On the other hand, uncontrolled beam loss arising from large-angle foil scattering was reduced drastically by the above efforts. While the original number of foil hits per particle was 41 with 100π-mm-mrad transverse painting, it was reduced to 15 by expanding the transverse painting area to 200π mm mrad, and further to 7 by optimizing the foil size and its position. This reduced number of foil hits expects that the machine activation near the charge-exchange foil is kept at less than 10 mSv/h on the chamber surface even for the 1-MW beam operation, which is sufficiently within the acceptable level.

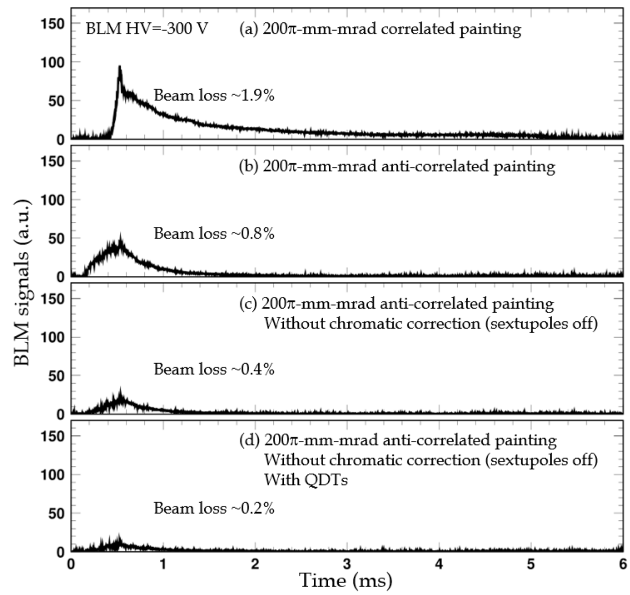

Figure 7: BLM signals at the collimator measured for the first 6 ms with a beam intensity of 1 MW.

SUMMARY

We restarted a 1-MW beam test in October, 2015 after the RF power supply upgrade.

By the recent efforts, the 1-MW beam operation is now estimated to be established within a permissible beam loss level. Though it is unfortunate that the routine output beam power from RCS is now limited to 200 kW due to a trouble of the mercury target, RCS beam commissioning is making steady progress toward realizing the routine 1-MW design beam operation.

The further parameter optimization for the 1-MW beam will be continued with more careful attention to beam quality as well as to beam loss.

REFERENCES

[1] H. Hotchi, Proc. of IPAC'15, p.1346.
[2] F. Tamura et al., PRST-AB **14**, 051004 (2011).
[3] M. Kinsho, in These Proceedings, TUXA01.
[4] H. Hotchi et al., PRST-AB **15**, 040402 (2012).
[5] F. Tamura et al., PRST-AB **12**, 041001 (2009).
[6] M. Yamamoto et al., NIM, A **621**, 15 (2010).
[7] H. Hotchi et al., NIM, A **778**, 102 (2015).
[8] H. Hotchi et al., PR-AB **19**, 010401 (2016).